Magnetic Evaluation of Mechanical Properties of High Silicon Quench and Tempered Steel

J N Mohapatra*, D Satish Kumar, G Balachandran

Research and Development, JSW Steel Limited, Vidyanagar, Toranagallu, Karnataka, India

ABSTRACT

A TRIP assisted steel was subjected to austenitization above Ac3 at 920°C to generate >98% martensite and inter critical austenization at 810°C to generate about 50% ferrite along with >48% martensite with retained austenite in both the case, tempered in the temperature range between 150 and 650°C. The former hardened and tempered steel show a fully tempered martensite while latter one shows significant ferrite coexisting with tempered martensite. In both conditions, superior mechanical properties (tensile toughness >20 GPa. %) were observed when tempered below 300°C. High Si, shifts the tempered martensite embrittlement to higher temperatures and suppresses the carbide formation and retains austenite laths within the tempered martensite that enhances properties. Magnetic hysteresis loop measurements were carried out at each stage and coercivity showed a strong correlation indicating precise non-destructive magnetic evaluation of tensile strength through a portable magnetic hysteresis loop tester.

Keywords: Quenched and Tempered Steel; Microstructure, Mechanical Properties, Magnetic properties; Non-Destructive Evaluation

INTRODUCTION

Automotive industry looks for the development of innovative microstructures in steels that can improve the strength and formability properties in flat products that have low carbon content (<0.25%). In view of this steel grades such as Dual phase steels, TRIP assisted steels, quench partitioned steels etc., have been developed. TRIP assisted steels are usually alloyed with elements such as Si or Al, which has a tendency to suppress the formation of carbides that resulted in residual austenite in the matrix during austenitization, followed by bainitic holding treatment or continuous cooling in the bainitic temperature range. DP steel on the other hand involves quenching from inter critical regime to form intercritical ferrite and carbon rich austenite which on quenching forms martensite in ferrite as the microstructure. The DP steel has poor local formability parameters such as whole expansion ratio due to the presence of brittle martensite in it. It is possible to subject a TRIP steel with high Si or Al content to dual phase heat treatment, where the presence of higher Si or Al content promotes retained austenite along with martensite that enhances the strength and ductility properties [1-3]. While all the above microstructures have been commercialized, there is very less insight into the investigation of quenching and tempering of a high Si TRIP steel from a fully austenitized condition, where along with martensite laths the retained austenite will be stabilized. Tempering decomposes martensite to ferrite and carbides still retaining some austenite. Thus, microstructure consisting of tempered martensite with retained austenite and carbides

is of interest to evaluate. It is possible that the TRIP steel subjected to a DP heat treatment cycle involving inter critical austenitization can also be tempered to improve the plastic properties of the steel. Here, along with tempered martensite there is likelihood of having softer ferrite along with tempered martensite which may enhance the plastic properties or formability of the steels. During tempering, Si atoms are rejected from the cementite to ferrite enhancing Si at interface for minutes a barrier to further carbide growth. Cementite has low Si solubility and diffusion is slow compared to carbon and controls the growth and coarsening of cementite. High tempering temperature and long holding required to precipitate carbides [4].

A medium carbon high Si, Ni-Cr-Mo steel on hardening retains austenite along martensite laths during quenching. Tempered martensite is found to be at 450°C. Tempering below 425°C, forms ε-carbides along with austenite along the laths. During TME, impurity elements such as phosphorus and antimony segregate to the prior austenite boundaries [5]. Heat treatment responses of tempering the martensite can be evaluated by studying the magnetic property of the materials [6-10]. The hardness and strength are related directly to the coercivity for the common pinning for the dislocations and magnetic domain wall motion. Thus, the variation in properties in the low alloy steel especially during hardening and tempering can be non-destructively evaluated through a non-destructive magnetic evaluation tester. In the present work, systematic studies were made on a lean alloyed 1.35% Si containing a low carbon TRIP assisted steel subjected to hardened

and tempering heat treatment. The austenitization was carried out at two different temperatures. In one set, austenitization was well above Ac3, which on hardening gave fully martensitic microstructure with retained austenite and in the second set austenitization was done in the intercritical range to deliberately introduce softer ferrite along with martensite on hardening. The microstructures, mechanical properties and magnetic properties of the steels were correlated in both the cases, post tempering between 150 and 650°C. Tempering the steel with intercritical ferrite and martensite (DP steel and DH steel) could be a favorable to improve the ductility and formability with marginal loss in strength.

MATERIALS AND METHODS

The steel used in the present study is a 3 mm thick hot rolled sheet produced at JSW Steel Limited, Vijayanagar Work. The steel was analyzed for its chemistry using SPECTRO make OES. Cut steel samples were subjected to two sets of heat treatments as shown schematically in Figure 1. One set of samples were austenitized at 920°C for 20 minutes and another set of samples were quenched from 810°C. Both the set of samples were tempered in the temperature range between 150°C and 650°C in an interval of 100°C with a holding time of 30 minutesutes. Magnetic hysteresis loop (MHL) measurements were carried out on the samples through a portable non-destructive magnetic evaluation devise (MagStar) at a magnetizing

field of 80 kA/m and magnetizing frequency of 50 mHz [11,12]. The hardened and tempered steel samples were subjected to mechanical property evaluation with ASTM E-8M sub size tensile specimens [13]. At every tempering temperature 3 samples were evaluated for the study. The tensile testing was conducted through a Zwick Make 250 kN tensile testing machine at 0.008/s strain rate. Optical microstructure was observed through an opto-digital Olympus make microscope and scanning electron microscopy was made through a Hitachi make SEM. The pseudobinary phase diagram of the steel as a function of temperature and carbon content was obtained through thermocalc software is shown in Figure 2.

RESULTS

The chemical composition of the steel with the transformation temperatures is shown in Table 1. The steel has 0.17 %C, which is good for weldability and formability of the steel. The steel has 1.72% Mn which decreases the A1 temperature that results in enlarged austenite fraction during austenitization. The steel has 0.02% Nb, 0.04% Ti and 0.06% Al, all of which ensures that the steel maintains a fine grained structure, during deformation and thermal treatments. The steel has 1.35% Si which shifts the tempered martensite embrittlement region to higher temperature range during tempering, which enhances the low temperature range where high strength and ductility can be retained.
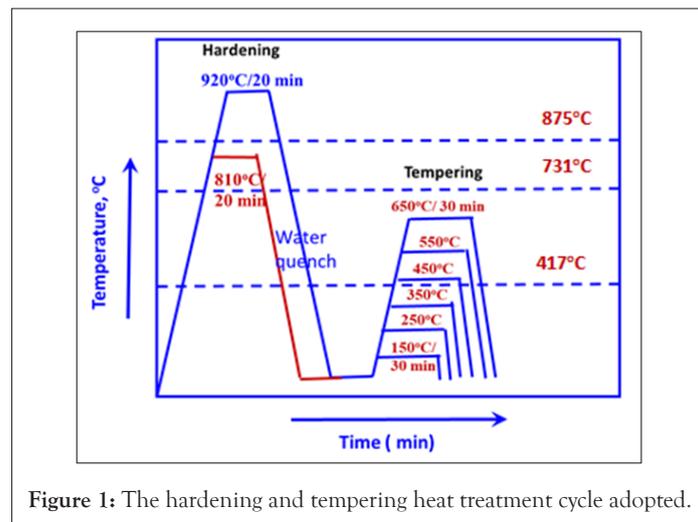

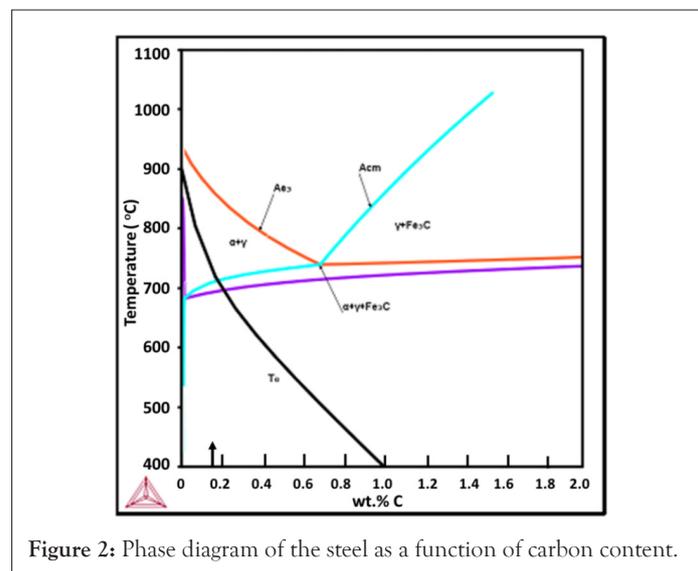**Figure 1:** The hardening and tempering heat treatment cycle adopted.

Figure 2: Phase diagram of the steel as a function of carbon content.

Table 1: Chemical composition (wt. %) and critical temperatures (˚C) of the steel studied.

C	Mn	Si	Nb	Ti	N	Al	S	P	A_{C1}	A_{C3}	Bs	Ms
0.17	1.72	1.35	0.02	0.04	0.005	0.06	0.003	0.016	731	875	557	417

The pseudobinary phase diagram of the steel, as evaluated by Thermocalc shows the phase distribution as a function of increasing carbin content. The given steel on hating to 920˚C forms austente completely, while heating the steel to 810˚C results in 47% ferrite and 53% austenite as per phase diagram.

Microstructure

The optical microstructure of the steel hardened from 920˚C with 20 minutes holding and after tempering typically at 250˚C, 450˚C and 650˚C is shown in Figure 3 along with their corresponding SEM micrographs. The microstructure shows lath martensitic in nature with high dislocation density in the as-quenched condition. Using Koinstein-Marbuerger equation the estimated fraction of martensite is 98.4% with retained austenite content <1.6%.

$$f_{QT}^m = 1-\exp\left(-1.1 \times 10^{-2} \,(Ms\text{-Quench Temperature})\right)\ldots\ldots\ldots\ldots\ldots(1)$$

Tempering up to 250˚C still retains the lath microstructure and the tempering reaction tends to precipitate fine epsilon carbides that cannot be resolved in optical or SEM microstructures [14]. Beyond 250˚C, the retained austenite decomposes in low alloy steels. In high Si steels, the carbide precipitation may be delayed, which benefits the strength and ductility [1-5].

Tempering at 450˚C, enable greater carbide precipitation and recovery of the structure with laths broadening. Thin streaks of carbide decorate at lath boundaries. Tempering above 500˚C, leads to the coarsening of the carbides and the carbon free equilibrium ferrite becomes coarsened as shown in the optical and the SEM microstructures in Figure 3. The optical and SEM microstructures of the steel intercritically austenitized at 810˚C for 20 minutes holding followed by quenching and tempering at 250˚C, 450˚C and 650˚C as shown in Figure 4. Theoretically, intercritical austenitization at 810˚C gives 47% ferrite content with austenite based on Figure 2. The measured free ferrite content was 49% from the microstructure. Tempering the intercritically austenitized steel samples tempers the martensite fraction formed on hardening. The microstructure of the steel tempered till 250˚C shows intercritical ferrite with tempered martensite with same morphology as that of as quenched samples. Tempering at 450˚C precipitates fine carbide along the lath boundaries. Tempering at 650˚C shows that the carbides are coarsened.

During the intercritical treatment, there is about 49% carbide free ferrite. As the carbon solubility in ferrite during inter critical heat treatment is lower, the equilibrium austenite is enriched with the carbon rejected by the ferrite. This carbon rich austenite forms a martensite which is stronger than the martensite without intercritical ferrite formation. Thus, a composite effect of hard and soft phases is built in the microstructure. Apart from this, during tempering, the carbides formed in the inter critically treated sample is likely to precipitate more in the martensite zones compared to the fully austenitized condition. Hence, the carbides in the tempered martensite microstructure, is likely to be more dense in the intercritically austenitized steel.

Mechanical properties

The mechanical properties such as yield strength, ultimate tensile strength, total elongation of the fully austenitized and intercritically austenitized steel with increase in tempering temperature is shown in Figure 5. The presence of the softer intercritical ferrite in the matrix has softened the steel than in the samples in fully austenitized condition. The strength value decreases with increasing tempering temperature. The loss in strength is very moderate till 350˚C. The ductility values are reasonably high till 300˚C. Hence, this condition can be exploited for ultrahigh strength application such as in automotive structures with light weighting opportunity. The tensile strength and the yield strength is higher for the fully austenite steel with maximum martensite content than the steels with softer intercritical ferrite. The ductility values pass through a minutesimum, at about 450˚C, as shown in Figure 5. This temperature corresponds to the tempered martensite embrittlement. This sort of embrittlement usually takes place in the conventional hardened and tempered low alloy steel at about 350˚C [3]. The presence of high Si content in the steel shifts the tempered martensite embrittlement to the higher tempering temperature of 450˚C [3]. Hence, the lowering of ductility is due to the embrittlement. Tempering the steel beyond 450˚C shows monotonic increase in ductility in the steel while the strength rapidly decreases. The strength values at 500 to 600˚C correspond to 1100 to 1000 MPa tensile strength with ductility 15 to 20% in fully austenitized steel. At higher tempering temperatures, the tensile strength of the fully austenitized steel and the intercritically annealed steel are very close above 550˚C tempering temperature although the yield strength of the fully austenitized and tempered steel is higher. Superior ductility of the intercritically austenitized steel is found at all tempering temperatures. The yield ratio and tensile toughness of the steels are shown in Figure 6. Higher yield ratio is found in the fully austenitized followed by water quenched steel compared to the inter critically annealed followed by water quenching the steel due to the presence of large amount of hard martensite phase. The yield ratio increased with tempering temperature in both the steels and gets saturated at higher tempering temperatures, greater than 500˚C. The tensile toughness is greater than 20 GPa% up to 300˚C tempering in both the steels and then decreased up to 450˚C and then although increased, remain below 20 GPa.% level. TRIP Steel subjected to DP steel heat treatment (intercritical annealing following water quenching) forms ferrite matrix with martensite and retained austenite. This is the condition when the present steel is water quenched before tempering. A mild heat treatment of tempering less than 300˚C give excellent strength and ductility compared to DH steel. The property range extends with tensile toughness beyond 20 GPa%. The work hardening behavior of the steels were assessed from the true stress-true strain diagram in Figure 7, using the Hollomon equation ($\sigma = k\,\varepsilon^n$) as shown in Figure 8. The slope in this figure is the n value and it is seen that the n-value initially is nearly same for all conditions. The work hardening initially proceeds in the ferrite matrix where the dislocations accumulate with increase in strain. At higher strains, the dislocations move to tempered martensite zones rich in carbides, where dislocation moves with difficulty.
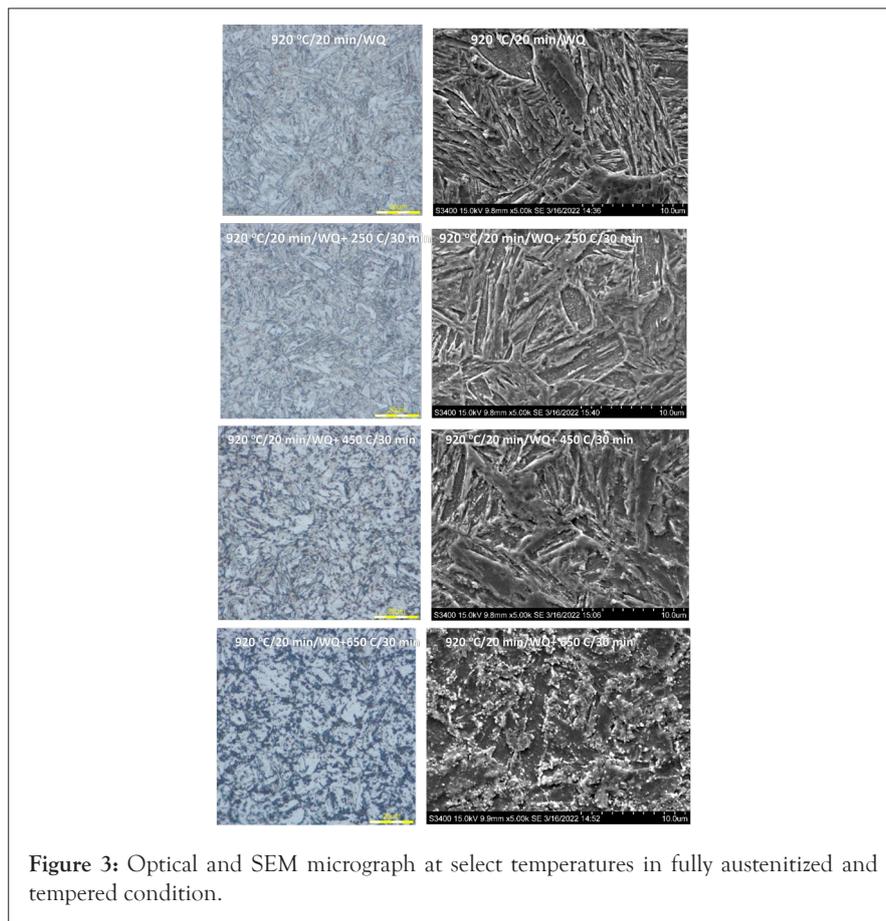
Figure 3: Optical and SEM micrograph at select temperatures in fully austenitized and tempered condition.
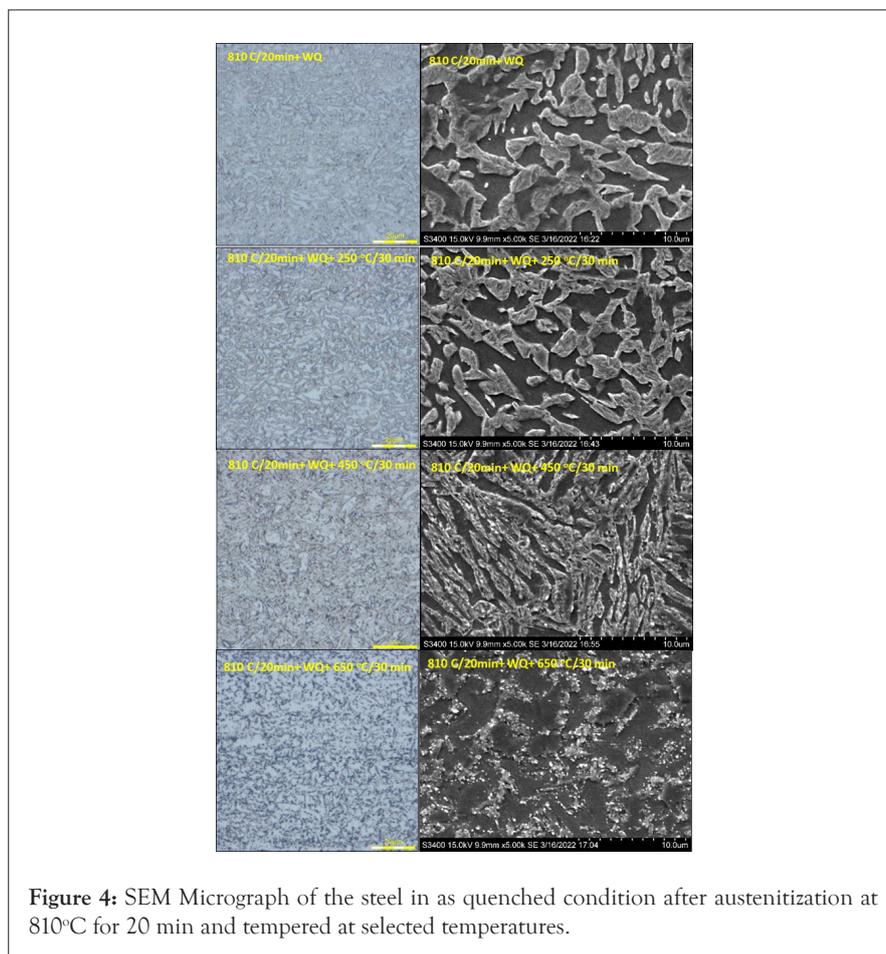
Figure 4: SEM Micrograph of the steel in as quenched condition after austenitization at 810°C for 20 min and tempered at selected temperatures.
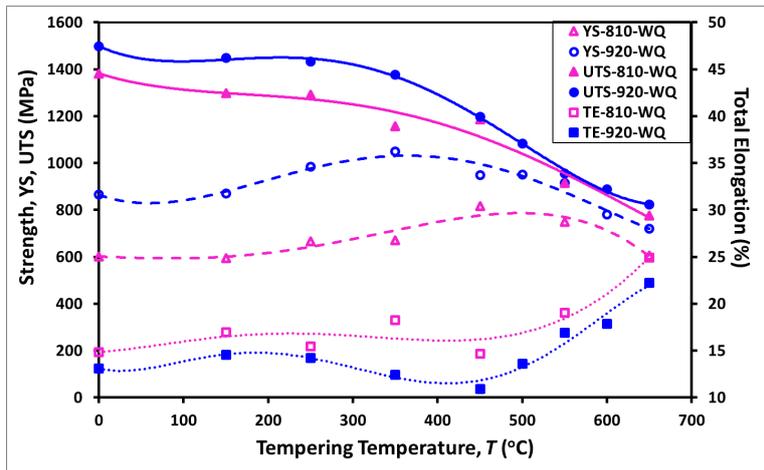
Figure 5: Yield Strength (YS), Ultimate Tensile Strength (UTS) and Total Elongation (TE) of the fully austenitized and IC austenitized steel with increase in tempering temperature.
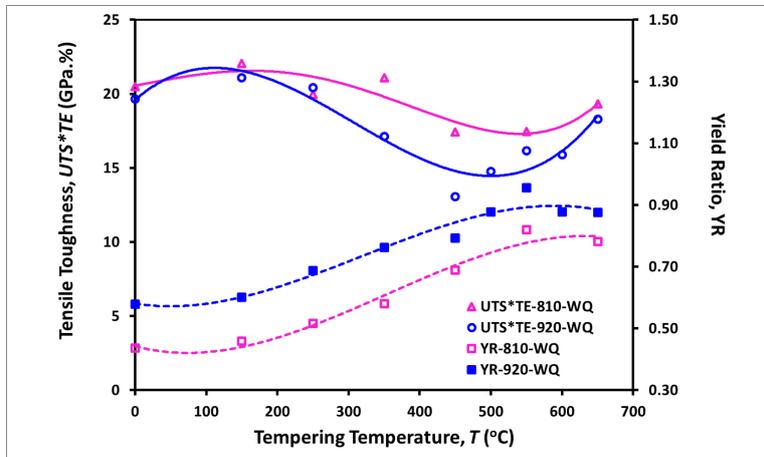

Figure 6: Yield ratio and the tensile toughness of the fully austenitized and intercritically austenitized and quenched steel as a function of tempering temperature.
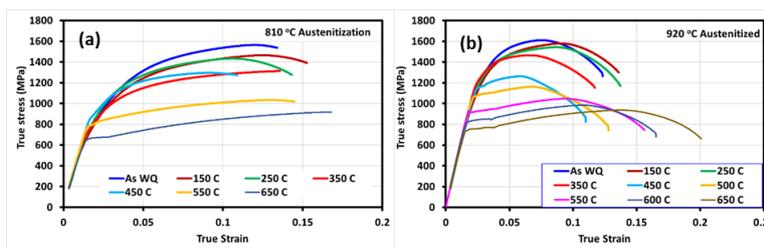

Figure 7: True stress - true strain curves of the steel hardened from (a) 810 oC and (b) 920 °C and tempered at various temperature.
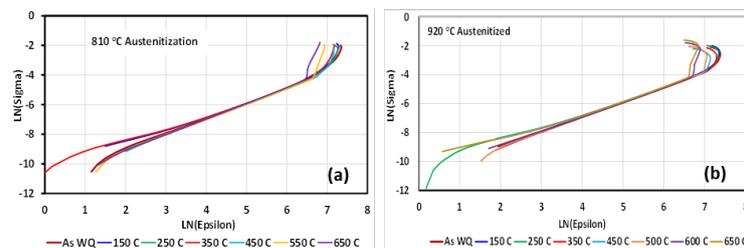

Figure 8: The work hardening behavior as per Hollomon equation (σ=K εn) (a) intercritical holding followed by tempering (b) Austenization Above Ar3 followed by tempering.

The work hardening characteristics have further been analysed using the modified Crussard-Jaoul (CJ) model, where the plastic strain during work hardening is related to the true stress as follows [15],

$$\varepsilon_p = \varepsilon_0 + C\sigma m \quad \text{.................(2)}$$

Where ε_p = actual plastic strain

ε_0 = initial true strain

σ = true stress

m= (1/n)

C= material constant

On logarithmic scale the equation becomes,

$$Ln\ (d\sigma/d\varepsilon_p) = (1 - m)\ ln\sigma\text{-}ln\ C_m \quad \text{................. (3)}$$

The plots so obtained from the above equation for austenitization at 810 and 920°C are shown in Figure 9. The change in slope is indicative of the change in deformation mechanism. In the initial stages dislocations are generated, move and accumulate in the softer ferrite phase. When the stress exceeds a critical level, the deformation takes place in the harder phases of tempered carbides. The rate of strain hardening decreases with increasing tempering temperatures. At similar tempering temperature, the strain hardening rate decreases for intercritically treated steel compared to the fully austenitized steel. From the equation (2) the (1-m) is a measure of the slopes in Figure 7. When the value (1/m) is high, higher strain hardening takes place. It is seen that higher strain hardening capability is realized in the Table 2.

Magnetic properties

The change in coercivity, remanence, and maximum induction of the steels with increase in tempering temperature is shown in Figure 10a. The coercivity decreased while maximum induction marginally increased with increase in tempering temperature while the remanence decreased up to 250°C and then increased. The as quenched steel from above A3 is having very high volume fraction of martensite along with high density of dislocations with lot of compressive residual stress. Hence the magnetic domain movement is restricted strongly leading to the higher value of coercivity of the steel in as-quenched condition. In the contrary the steel quenched after inter critical holding having almost 50% ferrite helps in easy movement of magnetic domain wall leading to relatively lower coercivity. With increase in tempering temperature the coercivity decrease in the fully austenized and quenched steel sharply due to the reduction in the residual stresses whereas in the inter critically austenized steel showed a slow decrease in the coercivity. Although at low temperature tempering fine epsilon carbide restricts the magnetic domains could lead to increase in coercivity, due to the large relaxation in the residual stress for the tempering of martensites overwhelm minutes the pinning by epsilon carbides and showed a decrease in trend with tempering. The maximum induction and remanence are higher in the intercritically austenized steel due to the presence of higher volume fraction of ferrite. The decrease in remanence up to 250°C is probably due to the precipitation of the finer epsilon carbides after which the coarsening of the carbides and increase in the inter carbide distance leads to the rapid increase in the remanence of the steels. The decrease in coercivity is also due to the coarsening of carbides and increase in the inter carbide distance which lead to decrease in the pinning density for the magnetic domain wall motion. As coercivity is increased with the strong pinning of the magnetic domain wall by density of dislocations or strain field of dislocation, carbides, secondary phases which are also restricts the dislocation movement leading to increase in tensile strength of the steels, correlation is expected between the two due to the common pinning points. Correlation of coercivity with the tensile strength of the steel is shown in Figure 10b. A strong correlation is found between the coercivity with the tensile strength of the steels (Equation-4) indicating that precise evaluation of the

tensile strength can be made by monitoring the coercivity of the steels through a non-destructive magnetic evaluation device.

$$UTS\ (MPa)=103.68*Hc\ (A/m)+155.2 \quad \text{............................ (4)}$$
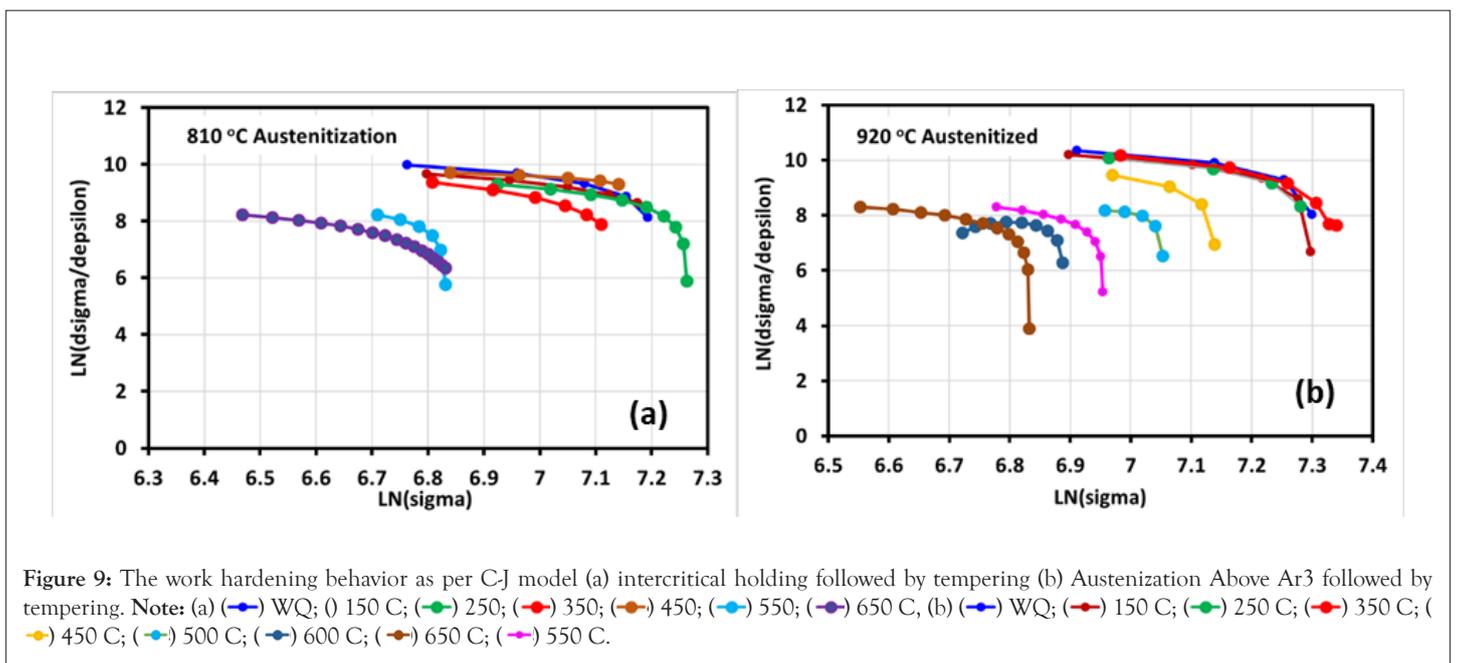
$$R^2=0.88$$

Figure 9: The work hardening behavior as per C-J model (a) intercritical holding followed by tempering (b) Austenization Above Ar3 followed by tempering. **Note:** (a) (⬤) WQ; () 150 C; (⬤) 250; (⬤) 350; (⬤) 450; (⬤) 550; (⬤) 650 C, (b) (⬤) WQ; (⬤) 150 C; (⬤) 250 C; (⬤) 350 C; (⬤) 450 C; (⬤) 500 C; (⬤) 600 C; (⬤) 650 C; (⬤) 550 C.

Table 2: The Work hardening characteristics at 920°C and 810°C.

Tempering Temperature		WQ	150	250	350	450	500	550	600	650	0.005
Austenitized at 920°C											
Stage 1	(1-m)	-2.04	-8.78	-2.28	-5.39	-4.44	5.17	-	5.17	-2.55	
	m	3.04	9.78	3.28	6.39	5.44	-4.17	-	-4.17	3.55	
	1/m	0.33	0.1	0.31	0.16	0.18	-0.24	-	-0.24	0.28	
	0.005	0.005	0.005	0.005	0.005	0.005	0.005	0.005	0.005	0.005	
Stage 2	(1-m)	1.63	-1.04	-17.68	-0.82	-11.76	-16.98	-	-1.08	-19.82	
	m	-0.63	2.04	18.68	1.82	12.76	17.98	-	2.08	20.82	
	1/m	-1.58	0.49	0.05	0.55	0.08	0.06	-	0.48	0.05	
Austenitized at 810°C											
Stage 1	(1-m)	-2.04	-3.91	-0.3	-2.81	-1.35	-	-0.4	-	-2.26	
	m	3.04	4.91	1.3	3.81	2.35	-	1.4	-	3.26	
	1/m	0.33	0.2	0.77	0.26	0.43	-	0.71	-	0.31	
Stage 2	(1-m)	-0.06	-13.24	-5.81	-0.01	-1.72	-	-9.93	-	-14.42	
	m	1.06	14.24	6.81	1.01	2.72	-	10.93	-	15.42	
	1/m	0.94	0.07	0.15	0.99	0.37	-	0.09	-	0.06	

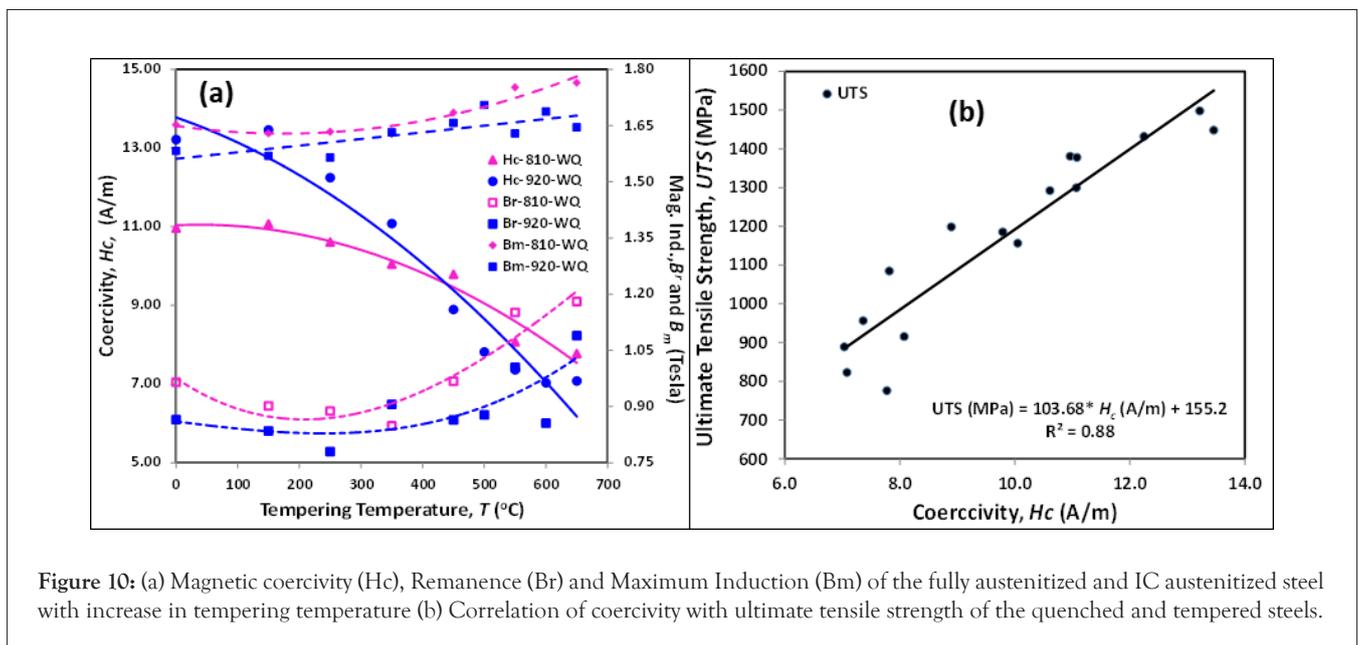**Figure 10:** (a) Magnetic coercivity (Hc), Remanence (Br) and Maximum Induction (Bm) of the fully austenitized and IC austenitized steel with increase in tempering temperature (b) Correlation of coercivity with ultimate tensile strength of the quenched and tempered steels.

CONCLUSION

A TRIP assisted steel with composition 0.17% C, 1.35 % Si, 1.72% Mn, microalloyed with Nb and Ti was subjected to a hardening heat treatment from above Ac3 temperature and from the inter critical heat treatment condition. The quenched samples were tempered at various tempering temperature between 150°C and 650°C.

The steel quenched and tempered with an austenitization temperature 920°C, which is above Ac3 showed completely martensitic laths with film type retained austenite between laths. Tempering below 300°C showed excellent strength in the range of 1400 MPa-1500 MPa and

elongations in the range of 13%-15%. The steel can be promoted for light weight applications in automotive structures. The same steel subjected to an inter critical heat treatment at 810°C followed by quenching and tempering at similar conditions introduced soft ferrite along with tempered martensite, which improved the ductility significantly with a loss in strength. The properties obtained on tempering below 300°C in both the ausenitization conditions showed tensile toughness greater than 20 GPa. %. In addition, the tempered martensite embrittlement was observed with a loss in ductility at 450°C in both the cases. The Si has shifted the tempered martensite that usually occurs at 350°C to 450°C. The study also brings out a

means to correlate the tempering response of the steel to its magnetic properties and there is a direct correlation between the coercivity and the tensile strength of the steel. Hence by monitoring coercivity the tensile strength of the tempered steel could be evaluated precisely.

Statements and declarations

REFERENCES

1. Nam WJ, Choi HC. Effect of Si on mechanical properties of low alloy steels. Mater Sci technol. 1999;15(5):527-530.

2. Sahoo G, Kumar P, Nageswaran K, Singh KK, Kumar V, Dhua SK. High-Si-Content Quenched and Tempered Steel for High-Strength Application. J Mater Eng Perform. 2021;30(12):9290-301.

3. Horn RM, Ritchie RO. Mechanisms of tempered martensite embrittlement in low alloy steels. Metall Trans A. 1978;9(8):1039-1053.

4. Chang L, Smith GD. The silicon effect in the tempering of martensite in steels. J phys Colloq. 1984;45(C9):C9-397.

5. Youngblood JL, Raghavan M. Microstructure and mechanical properties of quenched and tempered 300M steel. 1978.

6. Akujärvi V, Cedell T, Gutnichenko O, Jaskari M, Andersson M. Evolution of magnetic properties during tempering. Int J Adv Manuf Technol. 2022;119(3):2329-2339.

7. Kumar H, Mohapatra JN, Roy RK, Joseyphus RJ, Mitra A. Evaluation of tempering behaviour in modified 9Cr–1Mo steel by magnetic non-destructive techniques. J Mater Res Technol 2010;210(4):669-674.

8. Mohapatra JN, Mohanty S, Dabbiru SK, Tripathy I. Correlation of magnetic properties with mechanical properties of a high tensile grade steel in various heat treated conditions. Trans Indian Inst Met. 2018;71(10):2361-2374.

9. Mohapatra JN, Babu TS, Dabbiru SK, Balachandran G. Magnetic hysteresis loop as a tool for the evaluation of mechanical properties of hypoeutectoid pearlitic steels with spheroidization heat treatmemt. J Nondestr Eval. 2021;40(3):1-9.

10. Mohapatra JN, Kumar S, Akela AK, Prakash Rao S, Kaza M. Magnetic hysteresis loop as a tool for the evaluation of microstructure and mechanical properties of DP steels. J Mater Eng Perform. 2016;25(6):2318-25.

11. Mohapatra JN, Akela AK. Magnetic evaluation of tensile deformation behaviour of TRIP assisted steels. J Nondestr Eval. 2019;38(1):1-7.

12. Mohapatra JN, Dabbiru SK, Balachandran G. Magnetic Evaluation of Mechanical Properties of High Silicon Quenched and Tempered Steel. J N Mohapatra, D. Satish Kumar and G. Balachandran.

13. Kim J, Chung KH, Lee W, Kong J, Ryu H, Kim D, et al. Optimization of boost condition and axial feeding on tube bending and hydro-forming process considering formability and spring-back. Met Mater Int. 2009;15(5):863-876.

14. Bhadeshia H, Honeycombe R. Steels: microstructure and properties. Butterworth-Heinemann; 2017.

15. Kim JH, Lee T, Lee CS. Microstructural Influence on Stretch Flangeability of Ferrite–Martensite Dual-Phase Steels. Crystals. 2020;10(11):1022.